1 Basic Properties and Band Structure

1.1 Graphene Band Structure

Graphene is a two-dimensional structure of carbon atoms. Single-layer graphene consists of only one layer of carbon atoms. A carbon atom has six electrons occupying the $1s^2$, $2s^2$, $2p_x$, and $2p_y$ atomic orbitals. When carbon atoms are brought together, one electron from the $2s$ orbital is promoted to the $2p_z$ orbital for the formation of hybrid orbitals. In diamonds, the $2s$, $2p_x$, $2p_y$, and $2p_z$ orbitals are mixed to form four sp^3 hybrid orbitals for each carbon atom; therefore, each carbon atom is joined with four neighbors by overlapping their sp^3 hybrid orbitals. In graphite, instead of four sp^3 hybrid orbitals, three sp^2 hybrid orbitals are formed through mixing of the $2s$, $2p_x$, and $2p_y$ orbitals, while the fourth orbital remains as $2p_z$. Overlapping sp^2 hybrid orbitals from two adjacent atoms creates a strong σ *covalent bond* (C–C bond); these in-plane σ *bonds* connect each carbon atom to three neighbors. The remaining $2p_z$ orbitals of these carbon atoms form π *bonds*, which are responsible for binding carbon layers together in graphite. Because π bonds are much weaker than σ bonds, graphite has a low shear strength so that its carbon layers can be easily detached. For monolayer graphene, these nearly free π electrons are responsible for most of its experimentally observed electronic and optical properties. Because the Pauli exclusion principle requires that π electrons from different carbon atoms do not occupy the same state, the large number of closely packed carbon atoms in graphene causes degenerate energy levels to split into continuously distributed nondegenerate levels of allowed energy states, forming energy bands.

The real-space two-dimensional honeycomb lattice of graphene is shown in Figure 1.1(a). The distance between two neighboring carbon atoms in graphene is

$$a \approx 0.142 \text{ nm}. \tag{1.1}$$

The primitive lattice vectors are

$$\mathbf{a_1} = \sqrt{3}a\left(\frac{\sqrt{3}}{2}\hat{x} - \frac{1}{2}\hat{y}\right) \quad \text{and} \quad \mathbf{a}_2 = \sqrt{3}a\left(\frac{\sqrt{3}}{2}\hat{x} + \frac{1}{2}\hat{y}\right). \tag{1.2}$$

Therefore, the lattice constant is

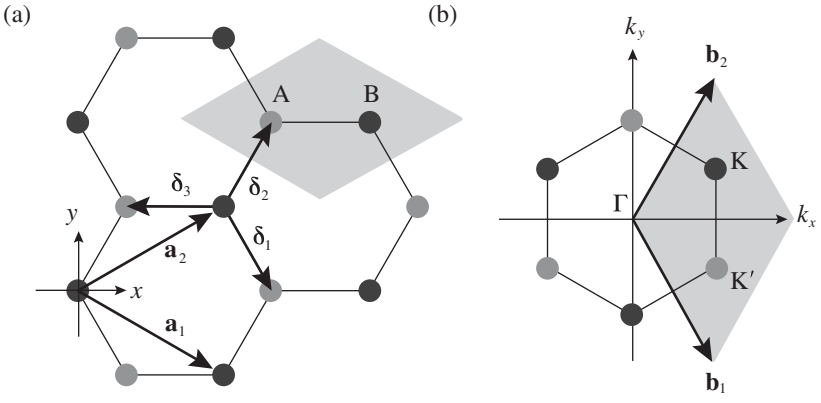

Figure 1.1 (a) Real-space honeycomb graphene lattice. The lattice consists of two overlapping Bravais sublattices, A (gray dots) and B (black dots). The primitive unit cell is drawn as a shaded area. $\mathbf{a}_1$ and $\mathbf{a}_2$ are the primitive lattice vectors. $\boldsymbol{\delta}_1$, $\boldsymbol{\delta}_2$, and $\boldsymbol{\delta}_3$ are vectors pointing from a B atom to its nearest A atoms. (b) Brillouin zone of graphene drawn as a shaded area. $\mathbf{b}_1$ and $\mathbf{b}_2$ are the primitive vectors of the reciprocal lattice. Dirac points K (black dots) and K′ (gray dots) are marked.

$$a_0 = |\mathbf{a_1}| = |\mathbf{a}_2| = \sqrt{3}a \approx 0.246 \text{ nm}. \tag{1.3}$$

The area A_p of a *primitive unit cell* can be obtained as

$$A_\mathrm{p} = |\mathbf{a}_1 \times \mathbf{a}_2 \cdot \mathbf{a}_3| = \frac{3\sqrt{3}}{2}a^2 = \frac{\sqrt{3}}{2}a_0^2, \tag{1.4}$$

where $\mathbf{a}_3 = \mathbf{a}_1 \times \mathbf{a}_2 / A_\mathrm{p} = \hat{z}$ is the unit vector that points in the direction perpendicular to the plane of the two-dimensional graphene lattice. We also find that the vectors connecting adjacent carbon atoms are

$$\boldsymbol{\delta}_1 = a\left(\frac{1}{2}\hat{x} - \frac{\sqrt{3}}{2}\hat{y}\right),\ \boldsymbol{\delta}_2 = a\left(\frac{1}{2}\hat{x} + \frac{\sqrt{3}}{2}\hat{y}\right), \text{ and } \boldsymbol{\delta}_3 = -a\hat{x}. \tag{1.5}$$

as shown in Figure 1.1(a).

The corresponding *Brillouin zone* of the lattice in Figure 1.1(a) is shown in Figure 1.1(b). The primitive vectors of the reciprocal lattice are

$$\begin{aligned} \mathbf{b_1} &= 2\pi \frac{\mathbf{a}_2 \times \mathbf{a}_3}{\mathbf{a}_1 \times \mathbf{a}_2 \cdot \mathbf{a}_3} = \frac{4\pi}{3a}\left(\frac{1}{2}\hat{x} - \frac{\sqrt{3}}{2}\hat{y}\right), \\ \mathbf{b}_2 &= 2\pi \frac{\mathbf{a}_3 \times \mathbf{a}_1}{\mathbf{a}_1 \times \mathbf{a}_2 \cdot \mathbf{a}_3} = \frac{4\pi}{3a}\left(\frac{1}{2}\hat{x} + \frac{\sqrt{3}}{2}\hat{y}\right). \end{aligned} \tag{1.6}$$

We can also find the vector $\mathbf{b}_3 = 2\pi \mathbf{a}_1 \times \mathbf{a}_2 / (\mathbf{a}_1 \times \mathbf{a}_2 \cdot \mathbf{a}_3) = 2\pi\hat{z}$ that is perpendicular to the plane of the two-dimensional reciprocal lattice. Therefore,

$$\mathbf{a}_i \cdot \mathbf{b}_j = 2\pi\delta_{ij}, \tag{1.7}$$

where δ_{ij} is the Kronecker delta function: $\delta_{ij} = 1$ if $i = j$, and $\delta_{ij} = 0$ if $i \neq j$.

The honeycomb lattice of graphene is not a *Bravais lattice* because the locations of all carbon atoms cannot be generated by the translation

$$\mathbf{R} = m\mathbf{a_1} + n\mathbf{a}_2, \tag{1.8}$$

where m and n are integers. The lattice structure of graphene consists of two overlapping *Bravais sublattices* A and B, and thus a primitive unit cell contains two carbon atoms, as shown in Figure 1.1(a). All of the carbon atoms on the same sublattice, but not those on the two different sublattices, are connected by the vector $\mathbf{R}$.

The electronic band structure of graphene can be obtained by using the *tight-binding model*. We start from a tight-binding Hamiltonian $\hat{H}$ for the Schrödinger equation:

$$\hat{H}\psi(\mathbf{r}) = E\psi(\mathbf{r}). \tag{1.9}$$

The wave function $\psi(\mathbf{r})$ is given by the linear superposition of orbital functions $\phi_l(\mathbf{r})$:

$$\psi(\mathbf{r}) = \frac{1}{\sqrt{N}}\sum_l c_l e^{i\mathbf{k}\cdot\mathbf{R}_l}\phi_l(\mathbf{r}) = \frac{1}{\sqrt{N}}\sum_l c_l e^{i\mathbf{k}\cdot\mathbf{R}_l}\phi(\mathbf{r}-\mathbf{R}_l), \tag{1.10}$$

where N is the number of unit cells, $\phi_l(\mathbf{r}) = \phi(\mathbf{r}-\mathbf{R}_l)$ is the ground state of the $2p_z$ electron of an isolated carbon atom that is located at $\mathbf{R}_l$, and the index l runs over all carbon atom points on the graphene lattice. Equation (1.10) is of the Bloch form because $\psi(\mathbf{r}+\mathbf{a}_i) = \exp(i\mathbf{k}\cdot\mathbf{a}_i)\psi(\mathbf{r})$, where $i = 1$ or 2. From the symmetry point of view, all atoms on sublattice A are geometrically identical; in other words, the surrounding is the same when viewing the graphene lattice from any atom on sublattice A. The same can be said for all atoms on sublattice B. No difference can be seen when viewing the graphene lattice from different atoms on the same sublattice. However, the atoms on sublattice A are not geometrically identical to those on sublattice B. By comparing the scenery in a certain direction, it is possible to tell the difference between viewing the graphene lattice from one atom on sublattice A and viewing it from one on sublattice B. Therefore, the wave function in (1.10) has only two independent coefficients for c_l: c_A and c_B, which respectively represent the amplitudes of the wave functions at carbon sites on sublattices A and B. Thus, (1.10) can be rewritten as a linear superposition of two Bloch functions ψ_A and ψ_B that are respectively wave functions for sublattices A and B:

$$\psi(\mathbf{r}) = c_\mathrm{A}\psi_\mathrm{A}(\mathbf{r}) + c_\mathrm{B}\psi_\mathrm{B}(\mathbf{r}) = \frac{c_\mathrm{A}}{\sqrt{N}}\sum_{l_\mathrm{A}} e^{i\mathbf{k}\cdot\mathbf{R}_{l_\mathrm{A}}}\phi_{l_\mathrm{A}}(\mathbf{r}) + \frac{c_\mathrm{B}}{\sqrt{N}}\sum_{l_\mathrm{B}} e^{i\mathbf{k}\cdot\mathbf{R}_{l_\mathrm{B}}}\phi_{l_\mathrm{B}}(\mathbf{r}), \tag{1.11}$$

where l_A and l_B run over all of the carbon atoms on sublattices A and B, respectively. The wave functions ψ_A and ψ_B are normalized, and the overlap of ψ_A and ψ_B is negligible [1], so that $\langle\psi_i|\psi_j\rangle = \delta_{ij}$. Therefore, $|\psi_\mathrm{A}\rangle$ and $|\psi_\mathrm{B}\rangle$ form the basis for the graphene wave functions.

By multiplying both sides of (1.9) by $\psi_\mathrm{A}^*(\mathbf{r})$, we obtain

$$c_\mathrm{A}\langle\psi_\mathrm{A}|\hat{H}|\psi_\mathrm{A}\rangle + c_\mathrm{B}\langle\psi_\mathrm{A}|\hat{H}|\psi_\mathrm{B}\rangle = c_\mathrm{A}E. \tag{1.12}$$

In (1.12), all of the interactions among A atoms and those between A atoms and B atoms are considered. However, it is very difficult to solve for the eigenenergy from (1.12) where all interactions are accounted for. To avoid such difficulty, (1.12) is simplified by taking the approximation of considering only the self-interaction of each carbon atom at a lattice point and the interactions of the atom with its three nearest neighbors; all long-range interactions are assumed to be much weaker than these interactions and are thus ignored. Within this approximation, (1.12) takes the simple form:

$$c_{\mathrm{A}}\langle\phi_{l_{\mathrm{A}}}|\hat{H}|\phi_{l_{\mathrm{A}}}\rangle + c_{\mathrm{B}}\langle\phi_{l_{\mathrm{A}}}|\hat{H}|\phi_{l_{\mathrm{B}}}\rangle(\mathrm{e}^{-\mathrm{i}\mathbf{k}\cdot\boldsymbol{\delta}_1} + \mathrm{e}^{-\mathrm{i}\mathbf{k}\cdot\boldsymbol{\delta}_2} + \mathrm{e}^{-\mathrm{i}\mathbf{k}\cdot\boldsymbol{\delta}_3}) = c_{\mathrm{A}}E. \tag{1.13}$$

By multiplying both sides of (1.11) by $\psi^*_{\mathrm{B}}(\mathbf{r})$ and taking the same approximation, we have

$$c_{\mathrm{B}}\langle\phi_{l_{\mathrm{B}}}|\hat{H}|\phi_{l_{\mathrm{B}}}\rangle + c_{\mathrm{A}}\langle\phi_{l_{\mathrm{B}}}|\hat{H}|\phi_{l_{\mathrm{A}}}\rangle(\mathrm{e}^{\mathrm{i}\mathbf{k}\cdot\boldsymbol{\delta}_1} + \mathrm{e}^{\mathrm{i}\mathbf{k}\cdot\boldsymbol{\delta}_2} + \mathrm{e}^{\mathrm{i}\mathbf{k}\cdot\boldsymbol{\delta}_3}) = c_{\mathrm{B}}E. \tag{1.14}$$

Equations (1.13) and (1.14) can be expressed in a matrix form for the eigenenergy equation of the system:

$$\begin{bmatrix} \varepsilon & -\gamma_0(\mathrm{e}^{-\mathrm{i}\mathbf{k}\cdot\boldsymbol{\delta}_1} + \mathrm{e}^{-\mathrm{i}\mathbf{k}\cdot\boldsymbol{\delta}_2} + \mathrm{e}^{-\mathrm{i}\mathbf{k}\cdot\boldsymbol{\delta}_3}) \\ -\gamma_0(\mathrm{e}^{-\mathrm{i}\mathbf{k}\cdot\boldsymbol{\delta}_1} + \mathrm{e}^{-\mathrm{i}\mathbf{k}\cdot\boldsymbol{\delta}_2} + \mathrm{e}^{-\mathrm{i}\mathbf{k}\cdot\boldsymbol{\delta}_3})^* & \varepsilon \end{bmatrix} \begin{bmatrix} c_{\mathrm{A}} \\ c_{\mathrm{B}} \end{bmatrix} = E \begin{bmatrix} c_{\mathrm{A}} \\ c_{\mathrm{B}} \end{bmatrix}, \tag{1.15}$$

where

$$\varepsilon = \langle\phi_{l_{\mathrm{A}}}|\hat{H}|\phi_{l_{\mathrm{A}}}\rangle = \langle\phi_{l_{\mathrm{B}}}|\hat{H}|\phi_{l_{\mathrm{B}}}\rangle \tag{1.16}$$

is the *self-interaction energy*, and

$$\gamma_0 = -\langle\phi_{l_{\mathrm{A}}}|\hat{H}|\phi_{l_{\mathrm{B}}}\rangle = -\langle\phi_{l_{\mathrm{B}}}|\hat{H}|\phi_{l_{\mathrm{A}}}\rangle \tag{1.17}$$

is the *nearest-neighbor hopping energy* in graphene. The nearest-neighbor hopping energy γ_0 is experimentally measured to have a value of $\gamma_0 = 3.16$ eV [2–4], which is the same as that found for graphite.

The nontrivial eigenvalues of (1.15) yield two eigenenergies:

$$E(\mathbf{k}) = \varepsilon \pm \gamma_0|\mathrm{e}^{\mathrm{i}\mathbf{k}\cdot\boldsymbol{\delta}_1} + \mathrm{e}^{\mathrm{i}\mathbf{k}\cdot\boldsymbol{\delta}_2} + \mathrm{e}^{\mathrm{i}\mathbf{k}\cdot\boldsymbol{\delta}_3}|, \tag{1.18}$$

where the plus sign is for the conduction band, which has higher energy, and the minus sign is for the valence band, which has lower energy. The conduction band and the valence band described by (1.18) are also called the π^* *band* and the π *band*, respectively. Equation (1.18) can be written in another form that is frequently seen in the literature [5,6]:

$$E(\mathbf{k}) = \varepsilon \pm \gamma_0\sqrt{3 + 2\cos(\sqrt{3}k_y a) + 4\cos\left(\frac{\sqrt{3}}{2}k_y a\right)\cos\left(\frac{3}{2}k_x a\right)}. \tag{1.19}$$

The energy band structure described by (1.19) is plotted in Figure 1.2(a). At the Γ point ($\mathbf{k} = 0$), we find the eigenenergies $E = \varepsilon \pm 3\gamma_0$ from (1.19), which are associated

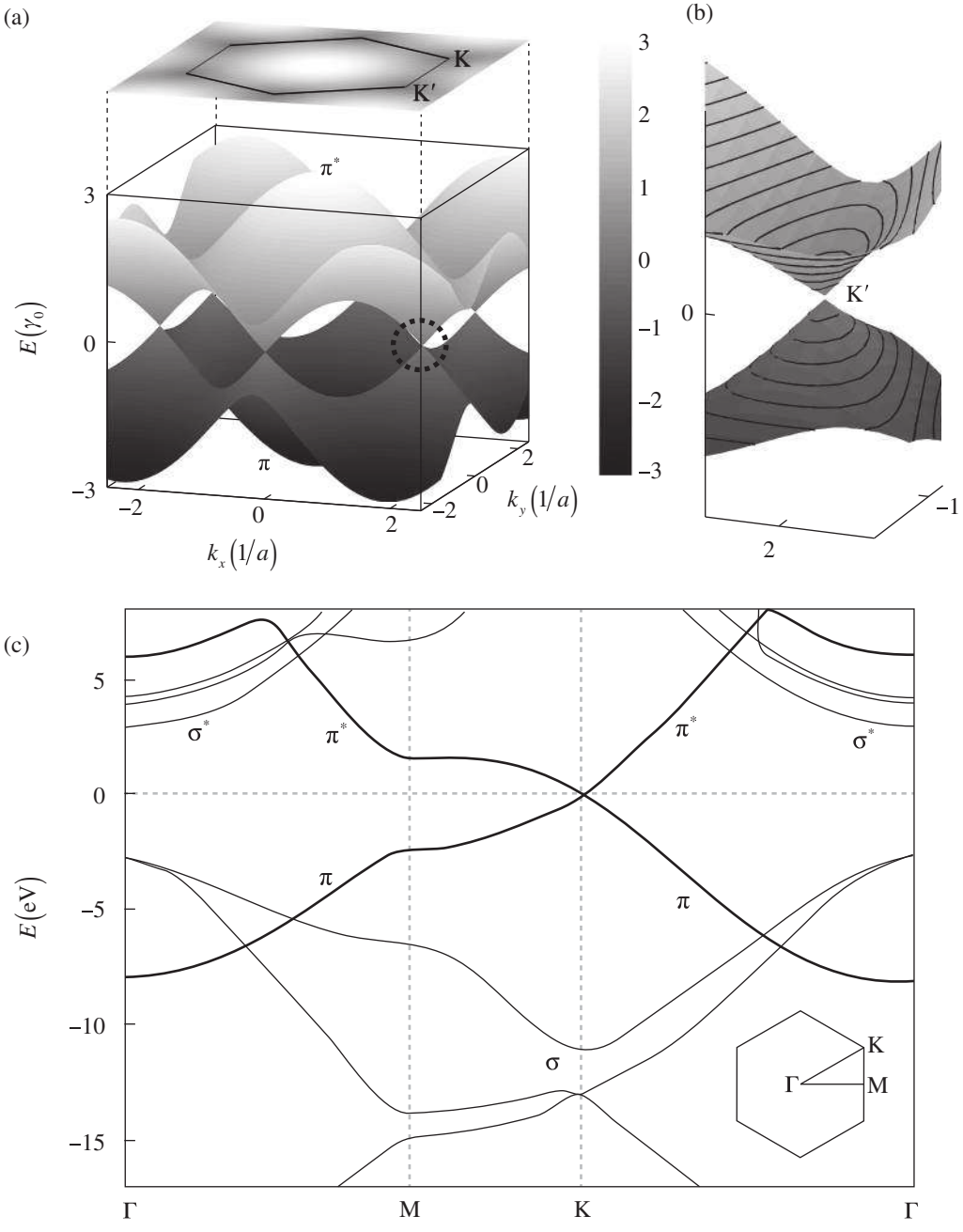

Figure 1.2 (a) Band structure of graphene plotted using (1.19) while setting the self-interaction energy to be $\varepsilon = 0$. The top surface of a higher energy is the conduction band (π^* band), and the bottom surface of a lower energy is the valence band (π band). The conduction band is projected onto a two-dimensional plane on the top. The circled region near the Dirac point K′ is enlarged in (b). (c) Full band structure of graphene. The thick curves are the π^* and π bands, and the thin curves are the σ^* and σ bands [7].

with the eigenstates $[c_A,\ c_B] = \frac{1}{\sqrt{2}}[1, \mp 1]$, respectively. The eigenenergy $E = \varepsilon - 3\gamma_0$ for the valence band is associated with symmetric bonding orbitals such that the amplitudes c_A and c_B of the wave functions for sublattices A and B have the same sign. By contrast, the eigenenergy $E = \varepsilon + 3\gamma_0$ for the conduction band is associated with antibonding orbitals such that the amplitudes c_A and c_B of the wave functions for sublattices A and B have opposite signs. An eigenstate of graphene is not necessarily bonding or antibonding, however; most eigenstates are a mixture of both bonding and antibonding orbitals. As we shall see in the following, only along a specific set of directions can the eigenstates be described by purely bonding or antibonding orbitals. The conduction band (π^* band) and the valence band (π band) are symmetric with respect to the $E = 0$ plane, as shown in Figure 1.2(a). Note that the long-range interactions of carbon atoms beyond the nearest neighbors are ignored in the above analysis. When these long-range interactions are accounted for, we find that the π^* and π bands are actually not symmetric to each other, as seen in Figure 1.2(c), where we also show the σ^* and σ bands contributed by the σ bonds.

As can be seen in Figure 1.2(a), the conduction band touches the valence band at $E = \varepsilon$. The self-interaction energy ε can be taken as the reference level by setting it to be 0 for simplicity so that an electron in a state on the conduction band has a positive energy and that in a state on the valence band has a negative energy. Then, (1.19) can be simplified as

$$E(\mathbf{k}) = \pm\gamma_0\sqrt{3 + 2\cos(\sqrt{3}k_y a) + 4\cos\left(\frac{\sqrt{3}}{2}k_y a\right)\cos\left(\frac{3}{2}k_x a\right)}, \qquad (1.20)$$

where the plus sign represents the conduction band and the minus sign represents the valence band. The points at $E(\mathbf{k}) = 0$ are called the *Dirac points*; the vicinities of these points are referred to as the valleys, where the graphene band structure can be described by the *relativistic Dirac equation*, which is further discussed in the following section. Corresponding to the two distinct sublattices A and B in the real space, there are two distinct groups of Dirac points K and K′ in the k space. Inside the Brillouin zone drawn in Figure 1.1(b), two Dirac points can be found at the k-space locations represented by the reciprocal space vectors:

$$\mathbf{K} = \frac{4\pi}{3\sqrt{3}a}\left(\frac{\sqrt{3}}{2}\hat{x} + \frac{1}{2}\hat{y}\right), \qquad \mathbf{K}' = \frac{4\pi}{3\sqrt{3}a}\left(\frac{\sqrt{3}}{2}\hat{x} - \frac{1}{2}\hat{y}\right). \qquad (1.21)$$

Another popular choice of the k-space locations of K and K′ in the literature is to select the K and K′ points on the k_y axis so that they are mirror symmetric with respect to the k_x axis; the physics and the results obtained in the following are unchanged by this alternative selection. It can be easily shown using (1.20) that $E(\mathbf{K}) = E(\mathbf{K}') = 0$ at these Dirac points.

For perfectly intrinsic graphene, the chemical potential, i.e., the Fermi level, is located at the energy level of the Dirac points, $E = 0$, so that the valence band is completely filled and the conduction band is completely empty. As most physics and carrier transitions happen at energy levels around the chemical potential, we shall rewrite

(1.20) by shifting the origin of the k space to one of the Dirac points and assume a small k to simplify (1.20). Substituting $\mathbf{k}$ in (1.20) with $\mathbf{K}+\mathbf{k}$ or $\mathbf{K}'+\mathbf{k}$, we obtain, for $|\mathbf{k}|a \ll 1$ in the vicinity of a Dirac point,

$$E = \pm\gamma_0\sqrt{\frac{9}{4}k_y^2a^2 + \frac{9}{4}k_x^2a^2} = \pm\frac{3}{2}a\gamma_0|\mathbf{k}| = \pm\hbar v_{\mathrm{F}}k, \tag{1.22}$$

where $\hbar$ is the reduced Planck's constant and

$$v_{\mathrm{F}} = \frac{3a\gamma_0}{2\hbar} \approx 1.0\times10^6\,\mathrm{m\,s^{-1}} \tag{1.23}$$

is the *Fermi velocity* in graphene, the physical meaning of which will become clear in Section 1.5. Equation (1.22) indicates that there is a region in the k space around each Dirac point where the carrier energy is linearly proportional to the wave number measured with respect to the given Dirac point. This region is called the *Dirac cone*, as shown in the insert in Figure 1.2(b). Because (1.22) can also be derived from the massless Dirac equation, electrons on the Dirac cone are also called *Dirac electrons*.

The Hamiltonian around the K point is obtained in the same way as (1.22) is obtained. By substituting $\mathbf{k}$ with $\mathbf{K}+\mathbf{k}$ in (1.15) to set the origin of the k space at the K point, the off-diagonal matrix elements for $|\mathbf{k}|a \ll 1$ become

$$\begin{aligned}\langle\psi_{\mathrm{A}}|\hat{H}_{\mathrm{K}}|\psi_{\mathrm{B}}\rangle &= -\gamma_0\left(\mathrm{e}^{-\mathrm{i}(\mathbf{K}+\mathbf{k})\cdot\boldsymbol{\delta}_1} + \mathrm{e}^{-\mathrm{i}(\mathbf{K}+\mathbf{k})\cdot\boldsymbol{\delta}_2} + \mathrm{e}^{-\mathrm{i}(\mathbf{K}+\mathbf{k})\cdot\boldsymbol{\delta}_3}\right)\\ &= \frac{\hbar v_{\mathrm{F}}}{2}\left[\sqrt{3}k_x + k_y + \mathrm{i}(k_x - \sqrt{3}k_y)\right]\end{aligned} \tag{1.24}$$

and

$$\langle\psi_{\mathrm{B}}|\hat{H}_{\mathrm{K}}|\psi_{\mathrm{A}}\rangle = \langle\psi_{\mathrm{A}}|\hat{H}_{\mathrm{K}}|\psi_{\mathrm{B}}\rangle^*. \tag{1.25}$$

The coefficients of k_x and k_y can be simplified by rotating both the k_x and k_y coordinate axes counterclockwise by 30 degrees through the unitary transformation

$$\begin{bmatrix}k_x'\\ k_y'\end{bmatrix} = \begin{bmatrix}\cos\frac{\pi}{6} & \sin\frac{\pi}{6}\\ -\sin\frac{\pi}{6} & \cos\frac{\pi}{6}\end{bmatrix}\begin{bmatrix}k_x\\ k_y\end{bmatrix} = \frac{1}{2}\begin{bmatrix}\sqrt{3}k_x + k_y\\ -k_x + \sqrt{3}k_y\end{bmatrix}. \tag{1.26}$$

Using (1.26), we obtain the relation $\langle\psi_{\mathrm{A}}|\hat{H}_{\mathrm{K}}|\psi_{\mathrm{B}}\rangle = \hbar v_{\mathrm{F}}(k_x' - \mathrm{i}k_y') = \langle\psi_{\mathrm{B}}|\hat{H}_{\mathrm{K}}|\psi_{\mathrm{A}}\rangle^*$ from (1.24) and (1.25). By dropping the prime symbols, $k_x' \to k_x$ and $k_y' \to k_y$, to simplify the notation, the Hamiltonian near the K point for $|\mathbf{k}|a \ll 1$ can be expressed as

$$\hat{H}_{\mathrm{K}} = \begin{bmatrix}0 & \hbar v_{\mathrm{F}}(k_x - \mathrm{i}k_y)\\ \hbar v_{\mathrm{F}}(k_x + \mathrm{i}k_y) & 0\end{bmatrix}. \tag{1.27}$$

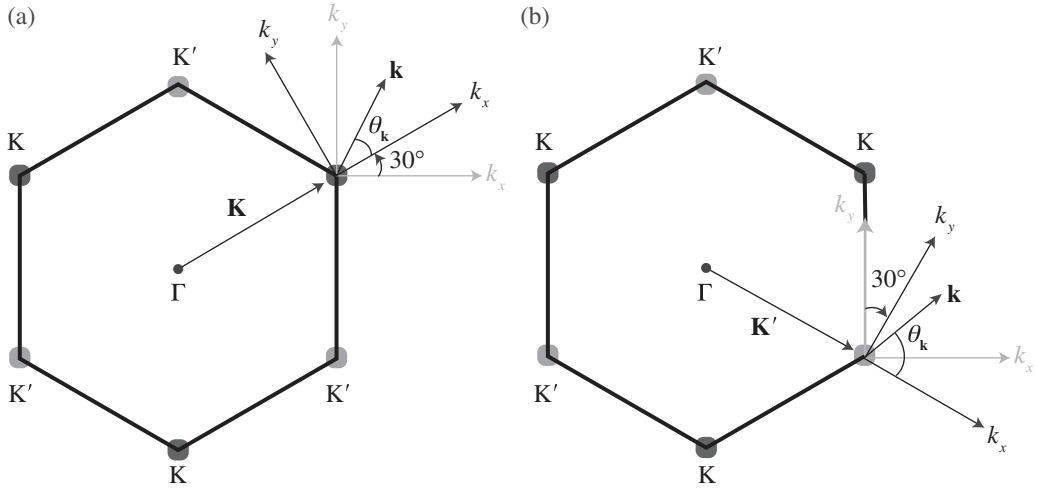

Figure 1.3 Wave vector $\mathbf{k}$ near (a) the K point, and (b) the K′ point. The Hamiltonian near the K or K′ point is obtained by rotating the coordinate from the gray axes to the black axes. The angle $\theta_\mathbf{k}$ is measured with respect to the rotated k_x axis.

The corresponding eigenfunctions are

$$\psi^{\mathrm{K}}_{\mathbf{k},\pm}(\mathbf{r}) = \frac{\mathrm{e}^{\mathrm{i}\mathbf{k}\cdot\mathbf{r}}}{\sqrt{2}}\begin{bmatrix} 1 \\ \pm\dfrac{k_x + \mathrm{i}k_y}{k} \end{bmatrix} = \frac{\mathrm{e}^{\mathrm{i}\mathbf{k}\cdot\mathbf{r}}}{\sqrt{2}}\begin{bmatrix} 1 \\ \pm\mathrm{e}^{\mathrm{i}\theta_\mathbf{k}} \end{bmatrix}, \tag{1.28}$$

where the $\pm$ signs correspond to the signs of the eigenenergies given in (1.22), and $\theta_\mathbf{k}$ is the polar angle measured between $\mathbf{k}$ and the rotated k_x axis as shown in Figure 1.3(a) for the K point.

Similarly, the Hamiltonian near the K′ point is obtained by substituting $\mathbf{k}$ with $\mathbf{K}' + \mathbf{k}$ in (1.15) and taking the unitary transformation by rotating the axes 30 degrees clockwise; the result for $|\mathbf{k}|a \ll 1$ is

$$\hat{H}_{\mathrm{K}'} = \begin{bmatrix} 0 & \hbar v_\mathrm{F}(k_x + \mathrm{i}k_y) \\ \hbar v_\mathrm{F}(k_x - \mathrm{i}k_y) & 0 \end{bmatrix} = \hat{H}^{\mathrm{T}}_{\mathrm{K}}. \tag{1.29}$$

The eigenfunctions are

$$\psi^{\mathrm{K}'}_{\mathbf{k},\pm}(\mathbf{r}) = \frac{\mathrm{e}^{\mathrm{i}\mathbf{k}\cdot\mathbf{r}}}{\sqrt{2}}\begin{bmatrix} \pm\mathrm{e}^{\mathrm{i}\theta_\mathbf{k}} \\ 1 \end{bmatrix}, \tag{1.30}$$

where the $\pm$ signs correspond to the signs of the eigenenergies given in (1.22), and $\theta_\mathbf{k}$ is the polar angle measured between $\mathbf{k}$ and the rotated k_x axis at the K′ point, as shown in Figure 1.3(b). From (1.28) and (1.30), it is clear that for the conduction band, the eigenstate is antibonding at $\theta_\mathbf{k} = \pi$ and bonding at $\theta_\mathbf{k} = 0$, as shown in Figure 1.4(a). By contrast, the eigenstate is bonding at $\theta_\mathbf{k} = \pi$ and antibonding at $\theta_\mathbf{k} = 0$ for the valence band, as shown in Figure 1.4(b).

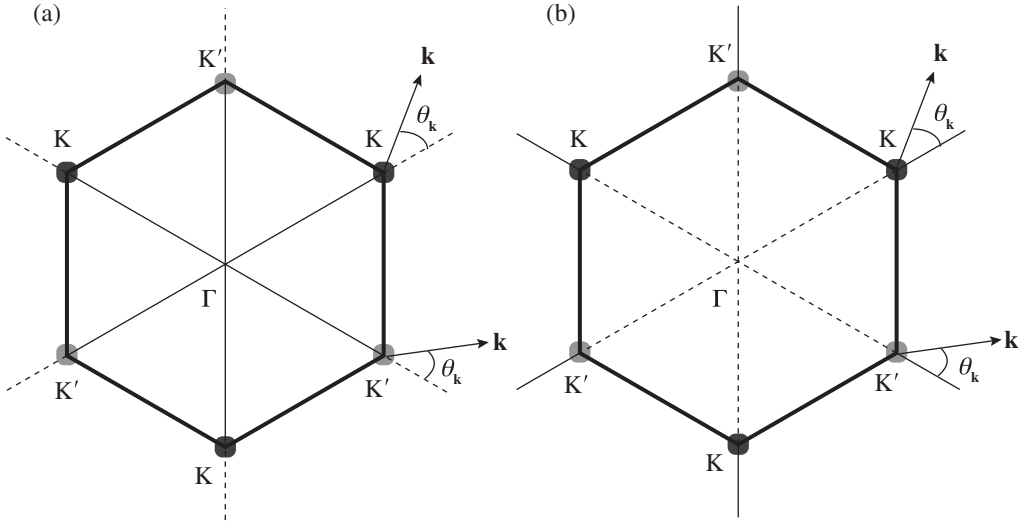

Figure 1.4 Antibonding (solid thin lines) and bonding (dotted lines) states in (a) the conduction band and (b) the valence band.

Equations (1.27) and (1.29) are often written as

$$\hat{H}_{\mathrm{K}} = v_{\mathrm{F}}\boldsymbol{\sigma}\cdot\mathbf{p} \tag{1.31}$$

for an electron near a K point and as

$$\hat{H}_{\mathrm{K}'} = v_{\mathrm{F}}\boldsymbol{\sigma}^{*}\cdot\mathbf{p} \tag{1.32}$$

for an electron near a K′ point, where $\mathbf{p} = \hbar\mathbf{k}$ and $\boldsymbol{\sigma}$ is the Pauli vector:

$$\boldsymbol{\sigma} = \begin{bmatrix} 0 & 1 \\ 1 & 0 \end{bmatrix}\hat{x} + \begin{bmatrix} 0 & -\mathrm{i} \\ \mathrm{i} & 0 \end{bmatrix}\hat{y} + \begin{bmatrix} 1 & 0 \\ 0 & -1 \end{bmatrix}\hat{z}. \tag{1.33}$$

Note that $\mathbf{p} = \hbar\mathbf{k} = \hbar(k_x\hat{x} + k_y\hat{y})$ with $k_z = 0$ for the π electrons in monolayer graphene because they only move through the graphene lattice on the xy plane of a monolayer graphene sheet.

In fact, the Hamiltonian of graphene near a K or K′ point has the form identical to that of a spin one-half particle in a magnetic field; its eigenfunctions are two-component spinors, as seen in (1.28) and (1.30). In the case of graphene, $\boldsymbol{\sigma}$ does not really represent an electronic spin, but a *pseudospin* that indicates the sublattice on which the electron is located. We can define a *helicity operator* $\hat{h} = \boldsymbol{\sigma}\cdot\mathbf{p}/p$ to find the projection of the momentum along the pseudospin direction; then it can be shown that $\hat{h}\psi^{\mathrm{K}}_{\mathbf{k},\pm} = \pm\psi^{\mathrm{K}}_{\mathbf{k},\pm}$. The positive sign gives positive helicity, meaning that the momentum of an electron on the conduction band is parallel to the pseudospin, whereas the negative sign gives negative helicity, meaning that the momentum of an electron on the valence band is

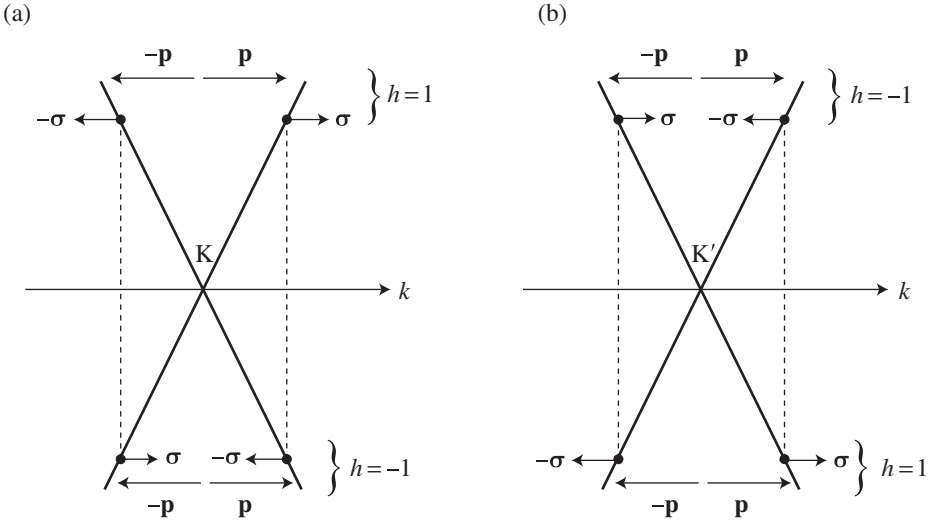

Figure 1.5 Helicity h, pseudospin $\boldsymbol{\sigma}$, and momentum $\mathbf{p}$ of an electron near (a) the K point, and (b) the K′ point. The directions of $\mathbf{p}$ and $\boldsymbol{\sigma}$ are shown. In the case of a hole, the direction of momentum is reversed. Due to the conservation of pseudospin, an electron or a hole cannot be scattered into an electron or a hole of a different pseudospin.

antiparallel to the pseudospin. The relation among the helicity, the carrier momentum, and the pseudospin are shown in Figure 1.5. Because of the conservation of pseudospin, a right-moving electron on the conduction band cannot be scattered into a left-moving electron on the conduction band or into a right-moving electron on the valence band. Such scattering requires the pseudospin to be flipped from $+1$ to -1 for an electron near the K point, or flipped from -1 to $+1$ for an electron near the K′ point, neither of which is allowed. Similarly, scattering of a left-moving electron on the conduction band into a right-moving electron on the conduction band or into a left-moving electron on the valence band is also forbidden. Nevertheless, such scattering events can happen when there exists a short-range potential that acts differently on sublattices A and B, thus breaking the symmetry between the two sublattices.

1.2 Density of States and Carrier Concentration

With the band structure near the Dirac point described by (1.22), the density of electron states of graphene in the energy range between E and $E + \mathrm{d}E$ for $E > 0$ near the conduction band edge is

$$\widetilde{\rho}_{\mathrm{c}}(E)\mathrm{d}E = \frac{1}{A}\sum_{\mathbf{k},\, E_{\mathbf{k}}>0} \delta(E_{\mathbf{k}} - E)\mathrm{d}E = \frac{g}{4\pi^2}\int_0^{\infty} \delta(\hbar v_{\mathrm{F}} k - E)2\pi k \mathrm{d}k\mathrm{d}E = \frac{2E}{\pi\hbar^2 v_{\mathrm{F}}^2}\mathrm{d}E, \tag{1.34}$$

and that for $E < 0$ near the valence band edge is